

DPPC Langmuir Monolayer at the Air–Water Interface: Probing the Tail and Head Groups by Vibrational Sum Frequency Generation Spectroscopy

Gang Ma and Heather C. Allen*

Department of Chemistry, The Ohio State University, 100 West 18th Avenue, Columbus, Ohio 43210

Received December 30, 2005. In Final Form: March 8, 2006

Dipalmitoylphosphatidylcholine (DPPC) is the predominant lipid component in lung surfactant. In this study, the Langmuir monolayer of deuterated dipalmitoylphosphatidylcholine (DPPC- d_{62}) in the liquid-expanded (LE) phase and the liquid-condensed (LC) phase has been investigated at the air–water interface with broad bandwidth sum frequency generation (BBSFG) spectroscopy combined with a Langmuir film balance. Four moieties of the DPPC molecule are probed by BBSFG: the terminal methyl (CD_3) groups of the tails, the methylene (CD_2) groups of the tails, the choline methyls (CH_3) in the headgroup, and the phosphate in the headgroup. BBSFG spectra of the four DPPC moieties provide information about chain conformation, chain orientation, headgroup orientation, and headgroup hydration. These results provide a comprehensive picture of the DPPC phase behavior at the air–water interface. In the LE phase, the DPPC hydrocarbon chains are conformationally disordered with a significant number of gauche configurations. In the LC phase, the hydrocarbon chains are in an all-trans conformation and are tilted from the surface normal by 25° . In addition, the orientations of the tail terminal methyl groups are found to remain nearly unchanged with the variation of surface area. Qualitative analysis of the BBSFG spectra of the choline methyl groups suggests that these methyl groups are tilted but lie somewhat parallel to the surface plane in both the LE and LC phases. The dehydration of the phosphate headgroup due to the LE–LC phase transition is observed through the frequency blue shift of the phosphate symmetric stretch in the fingerprint region. In addition, implications for lung surfactant function from this work are discussed.

Introduction

Lung surfactant is a complex mixture of lipids and proteins that forms a monolayer at the air–alveolus interface. The major function of lung surfactant is to lower the surface tension at the alveolar surface to near-zero values during exhalation, consequently easing the work of breathing and preventing the collapse of the lung.^{1–4} Lung surfactant is an essential material for life. Deficiency and dysfunction of lung surfactant contribute to the pathophysiology of several severe lung disorders such as respiratory distress syndrome (RDS) and acute respiratory distress syndrome (ARDS).⁴ Deficiency of lung surfactant in premature infants results in RDS, also known as Hyaline membrane disease.⁵ In the U.S., about 50,000–60,000 infants are at risk for RDS each year.⁴ Current clinical treatment for RDS is through surfactant replacement therapy, namely, the administration of exogenous surfactants.⁶ The rational design of effective exogenous surfactants is a major motivation in lung surfactant research. Dysfunction of lung surfactant is a condition associated with ARDS. ARDS results from lung injury and can affect patients of all ages including infants, children, and adults. Surfactant replacement therapy has been applied to ARDS, but it is less successful than surfactant replacement therapy in RDS because of the complex pathology of ARDS.⁴

A fundamental understanding of lung surfactant function can lead to a more effective and optimal therapy to treat lung

disorders.^{4,7} Numerous studies on a variety of lung surfactant model systems have been performed with a variety of physicochemical approaches including film balance,^{8–12} a captive bubble apparatus,^{13–17} a pulsating bubble surfactometer,¹⁸ fluorescence microscopy,^{11,19–33} Brewster angle microscopy (BAM),^{21,22,27,30–32,34–36} atomic force microscopy (AFM),^{25,26,33,36,37}

* Corresponding author. E-mail: allen@chemistry.ohio-state.edu.

(1) Schurch, S.; Goerke, J.; Clements, J. A. *Proc. Natl. Acad. Sci. U.S.A.* **1976**, *73*, 4698.

(2) Schurch, S.; Goerke, J.; Clements, J. A. *Proc. Natl. Acad. Sci. U.S.A.* **1978**, *75*, 3417.

(3) Goerke, J. *Biochim. Biophys. Acta* **1998**, *1408*, 79.

(4) Notter, R. H. *Lung Surfactants: Basic Science and Clinical Applications*; Marcel Dekker: New York, 2000.

(5) Avery, M. E.; Mead, J. *Am. J. Dis. Child.* **1959**, *97*, 517.

(6) Robertson, B.; Halliday, H. L. *Biochim. Biophys. Acta* **1998**, *1408*, 346.

(7) Creuwels, L. A. J. M.; Van Golde, L. M. G.; Haagsman, H. P. *Lung* **1997**, *175*, 1.

(8) Tabak, S. A.; Notter, R. H.; Ultman, J. S.; Dinh, S. M. *J. Colloid Interface Sci.* **1977**, *60*, 117.

(9) Notter, R. H.; Tabak, S. A.; Mavis, R. D. *J. Lipid Res.* **1980**, *21*, 10.

(10) Wang, Z.; Hall, S. B.; Notter, R. H. *J. Lipid Res.* **1995**, *36*, 1283.

(11) Ma, J.; Koppenol, S.; Yu, H.; Zograf, G. *Biophys. J.* **1998**, *74*, 1899.

(12) Longo, M. L.; Bisagno, A. M.; Zasadzinski, J. A.; Bruni, R.; Waring, A. *J. Science* **1993**, *261*, 453.

(13) Schurch, S.; Green, F. H.; Bachofen, H. *Biochim. Biophys. Acta* **1998**, *1408*, 180.

(14) Crane, J. M.; Putz, G.; Hall, S. B. *Biophys. J.* **1999**, *77*, 3134.

(15) Crane, J. M.; Hall, S. B. *Biophys. J.* **2001**, *80*, 1863.

(16) Zuo, Y. Y.; Gitiyfroz, R.; Acosta, E.; Policova, Z.; Cox, P. N.; Hair, M. L.; Neumann, A. W. *Langmuir* **2005**, *21*, 10593.

(17) Smith, E. C.; Crane, J. M.; Laderas, T. G.; Hall, S. B. *Biophys. J.* **2003**, *85*, 3048.

(18) Chang, C.-H.; Coltharp, K. A.; Park, S. Y.; Franses, E. I. *Colloids Surf., A* **1996**, *114*, 185.

(19) Lipp, M. M.; Lee, K. Y.; Zasadzinski, J. A.; Waring, A. *J. Science* **1996**, *273*, 1196.

(20) Nag, K.; Perez-Gil, J.; Cruz, A.; Keough, K. M. W. *Biophys. J.* **1996**, *71*, 246.

(21) Lipp, M. M.; Lee, K. Y. C.; Waring, A.; Zasadzinski, J. A. *Biophys. J.* **1997**, *72*, 2783.

(22) Lipp, M. M.; Lee, K. Y. C.; Zasadzinski, J. A.; Waring, A. *J. Rev. Sci. Instrum.* **1997**, *68*, 2574.

(23) Nag, K.; Perez-Gil, J.; Ruano, M. L.; Worthman, L. A.; Stewart, J.; Casals, C.; Keough, K. M. *Biophys. J.* **1998**, *74*, 2983.

(24) Kruger, P.; Schalke, M.; Wang, Z.; Notter, R. H.; Dluhy, R. A.; Losche, M. *Biophys. J.* **1999**, *77*, 903.

(25) Takamoto, D. Y.; Lipp, M. M.; Von Nahmen, A.; Lee, K. Y. C.; Waring, A. J.; Zasadzinski, J. A. *Biophys. J.* **2001**, *81*, 153.

(26) Ding, J.; Takamoto, D. Y.; von Nahmen, A.; Lipp, M. M.; Lee, K. Y.; Waring, A. J.; Zasadzinski, J. A. *Biophys. J.* **2001**, *80*, 2262.

(27) Bringezu, F.; Ding, J.; Brezesinski, G.; Zasadzinski, J. A. *Langmuir* **2001**, *17*, 4641.

grazing incidence X-ray diffraction (GIXD),^{27,33,35,38–40} attenuated total reflectance FTIR (ATR-FTIR),^{41,42} infrared reflection–absorption spectroscopy (IRRAS),^{43–51} and computer simulation.^{52–56}

Endogenous lung surfactant contains about 90 wt % lipids and 10 wt % surfactant proteins.^{4,7,57} Dipalmitoylphosphatidylcholine (DPPC) is the major lipid component in lung surfactant and accounts for about 40 wt % of mammalian lung surfactant. It is generally accepted that DPPC is responsible for the near-zero surface tension at the alveolar surface at the end of exhalation. The near-zero surface tension, an essential lung surfactant property, is probably due to the fact that DPPC can form a highly packed semicrystalline structure at the alveolar surface film at the end of exhalation.^{4,7,57} In addition to the significance of the existence of a large amount of DPPC in lung surfactant, the synergy between DPPC and other lipids and proteins is also crucial for proper lung surfactant function. Other lipids (e.g., unsaturated phospholipids, anionic phospholipids) and proteins (SP–B and SP–C) are believed to facilitate the respreading and adsorption of DPPC and help to produce a uniform force throughout the lung during the breathing cycle.^{4,7,57}

Our knowledge about lung surfactant function has been significantly expanded in recent years, yet many intriguing questions remain unanswered. Three open questions related to the interfacial structures of lung surfactant are given as examples.

(28) Piknova, B.; Schief, W. R.; Vogel, V.; Discher, B. M.; Hall, S. B. *Biophys. J.* **2001**, *81*, 2172.

(29) Kruger, P.; Baatz, J. E.; Dluhy, R. A.; Losche, M. *Biophys. Chem.* **2002**, *99*, 209.

(30) Discher, B. M.; Maloney, K. M.; Schief, W. R.; Grainger, D. W.; Vogel, V.; Hall, S. B. *Biophys. J.* **1996**, *71*, 2583.

(31) Discher, B. M.; Schief, W. R.; Vogel, V.; Hall, S. B. *Biophys. J.* **1999**, *77*, 2051.

(32) Schief, W. R.; Antia, M.; Discher, B. M.; Hall, S. B.; Vogel, V. *Biophys. J.* **2003**, *84*, 3792.

(33) Alonso, C.; Alig, T.; Yoon, J.; Bringezu, F.; Warriner, H.; Zasadzinski, J. A. *Biophys. J.* **2004**, *87*, 4188.

(34) Grigoriev, D.; Miller, R.; Wuestneck, R.; Wuestneck, N.; Pison, U.; Møhwald, H. *J. Phys. Chem. B* **2003**, *107*, 14283.

(35) Bringezu, F.; Ding, J.; Brezesinski, G.; Waring, A. J.; Zasadzinski, J. A. *Langmuir* **2002**, *18*, 2319.

(36) Ding, J.; Doudevski, I.; Warriner, H. E.; Alig, T.; Zasadzinski, J. A.; Waring, A. J.; Sherman, M. A. *Langmuir* **2003**, *19*, 1539.

(37) Flanders, B. N.; Vickery, S. A.; Dunn, R. C. *J. Microsc.* **2001**, *202*, 379.

(38) Lee, K. Y. C.; Gopal, A.; von Nahmen, A.; Zasadzinski, J. A.; Majewski, J.; Smith, G. S.; Howes, P. B.; Kjaer, K. *J. Chem. Phys.* **2002**, *116*, 774.

(39) Lee, K. Y. C.; Majewski, J.; Kuhl, T. L.; Howes, P. B.; Kjaer, K.; Lipp, M. M.; Waring, A. J.; Zasadzinski, J. A.; Smith, G. S. *Biophys. J.* **2001**, *81*, 572.

(40) Alonso, C.; Bringezu, F.; Brezesinski, G.; Waring, A. J.; Zasadzinski, J. A. *Langmuir* **2005**, *21*, 1028.

(41) Chung, J. B.; Hanneemann, R. E.; Franses, E. I. *Langmuir* **1990**, *6*, 1647.

(42) Williams, A. D.; Wilkin, J. M.; Dluhy, R. A. *Mikrochim. Acta Suppl.* **1997**, *14*, 687.

(43) Dluhy, R. A.; Reilly, K. E.; Hunt, R. D.; Mitchell, M. L.; Mautone, A. J.; Mendelsohn, R. *Biophys. J.* **1989**, *56*, 1173.

(44) Pastrana-Rios, B.; Flach, C. R.; Brauner, J. W.; Mautone, A. J.; Mendelsohn, R. *Biochemistry* **1994**, *33*, 5121.

(45) Mendelsohn, R.; Brauner, J. W.; Gericke, A. *Annu. Rev. Phys. Chem.* **1995**, *46*, 305.

(46) Cai, P.; Flach, C. R.; Mendelsohn, R. *Biochemistry* **2003**, *42*, 9446.

(47) Wang, L.; Cai, P.; Galla, H.-J.; He, H.; Flach, C. R.; Mendelsohn, R. *Eur. Biophys. J.* **2005**, *34*, 243.

(48) Shanmukh, S.; Howell, P.; Baatz, J. E.; Dluhy, R. A. *Biophys. J.* **2002**, *83*, 2126.

(49) Brockman, J. M.; Wang, Z.; Notter, R. H.; Dluhy, R. A. *Biophys. J.* **2003**, *84*, 326.

(50) Flach, C. R.; Cai, P.; Dieudonne, D.; Brauner, J. W.; Keough, K. M. W.; Stewart, J.; Mendelsohn, R. *Biophys. J.* **2003**, *85*, 340.

(51) Shanmukh, S.; Biswas, N.; Waring, A. J.; Walther, F. J.; Wang, Z.; Chang, Y.; Notter, R. H.; Dluhy, R. A. *Biophys. Chem.* **2005**, *113*, 233.

(52) Kaznessis, Y. N.; Kim, S.; Larson, R. G. *J. Mol. Biol.* **2002**, *322*, 569.

(53) Kaznessis, Y. N.; Larson, R. G. In *Lung Surfactant Function and Disorder*; Nag, K., Ed.; Taylor & Francis Group: Boca Raton, FL, 2005; p 229.

(54) Lee, H.; Kandasamy, S. K.; Larson, R. G. *Biophys. J.* **2005**, *89*, 3807.

(55) Kandasamy, S. K.; Larson, R. G. *Biophys. J.* **2005**, *88*, 1577.

(56) Freitas, J. A.; Choi, Y.; Tobias, D. J. *Biophys. J.* **2003**, *84*, 2169.

(57) Veldhuizen, R.; Nag, K.; Orgeig, S.; Possmayer, F. *Biochim. Biophys. Acta* **1998**, *1408*, 90.

First, recent studies of various lung surfactant model systems using microscopic techniques have shown that the physical state of lung surfactant at the air–water interface is more than a monolayer. Surface-associated multilayer structures can exist under both low and high surface pressures.^{24,25,33,47,58} The existence of these multilayer domains is believed to facilitate the spreading and adsorption properties of lung surfactant, yet there is little evidence of the actual structure and composition of these multilayer domains.^{59,60} Second, SP–B is thought to facilitate the respreading of DPPC during inhalation. However, the lipid–protein interaction mechanism is still unclear. Recent computer simulations have shown interesting results for the possible interaction mechanism between SP–B and DPPC,^{52,53,55} yet experimental evidence is still lacking. Third, it has been generally accepted that the formation of a DPPC-enriched film is necessary to produce near-zero surface tension during exhalation. The formation of the DPPC-enriched film requires some type of surface refinement during compression,^{61,62} though researchers have argued against this classical concept and have postulated a supercompressed fluid model.^{15,17,63} In this model, surface refinement becomes unnecessary, and a metastable structure accounts for the high surface pressure upon compression.⁶³ However, there is currently no structural or spectroscopic evidence to support this model. To answer these challenging questions, a fundamental understanding of the interfacial structure of DPPC is needed, as discussed further in this article.

Langmuir monolayers containing either pure components or mixtures of lung surfactant components have been widely used as model systems in fundamental research of the lung surfactant.^{4,64} The monomolecular insoluble monolayer at the air–water interface is an excellent model system to mimic some of the lung surfactant properties in vitro, such as the surface-tension-lowering ability during exhalation and the respreading ability during inhalation. Surface pressure, surface density, subphase pH, and subphase ionic strength can be easily controlled in this model system.

The study reported here investigates a model Langmuir monolayer of DPPC. A surface-selective vibrational spectroscopic technique, sum frequency generation (SFG) spectroscopy, combined with Langmuir film balance is used. SFG is a surface vibrational technique based on a second-order nonlinear process. Since its inception in 1987,^{65–67} SFG surface spectroscopy has been widely used to study a variety of interfacial phenomena and processes.^{68–72} Previous SFG investigations on DPPC Langmuir

(58) von Nahmen, A.; Schenk, M.; Sieber, M.; Amrein, M. *Biophys. J.* **1997**, *72*, 463.

(59) Galla, H. J.; Bourdos, N.; Von Nahmen, A.; Amrein, M.; Sieber, M. *Thin Solid Films* **1998**, *327–329*, 632.

(60) Bourdos, N.; Kollmer, F.; Benninghoven, A.; Ross, M.; Sieber, M.; Galla, H. J. *Biophys. J.* **2000**, *79*, 357.

(61) Goerke, J.; Clements, J. A. In *Handbook of Physiology: The Respiratory System*; Mackel, P. T., Mead, J., Eds.; American Physiology Society: Washington, DC, 1986; Vol. III, p 247.

(62) Keough, K. M. W. In *Pulmonary Surfactant: From Molecular Biology To Clinical Practice*; Robertson, B., Van Golde, L. M. G., Batenburg, J. J., Eds.; Elsevier: Amsterdam, 1992; p 109.

(63) Rugonyi, S.; Hall, S. B. In *Lung Surfactant Function and Disorder*; Nag, K., Ed.; Taylor & Francis Group: Boca Raton, FL, 2005; p 173.

(64) Zasadzinski, J. A.; Ding, J.; Warriner, H. E.; Bringezu, F.; Waring, A. J. *Curr. Opin. Colloid Interface Sci.* **2001**, *6*, 506.

(65) Hunt, J. H.; Guyot-Sionnest, P.; Shen, Y. R. *Chem. Phys. Lett.* **1987**, *133*, 189.

(66) Zhu, X. D.; Suhr, H.; Shen, Y. R. *Phys. Rev. B* **1987**, *35*, 3047.

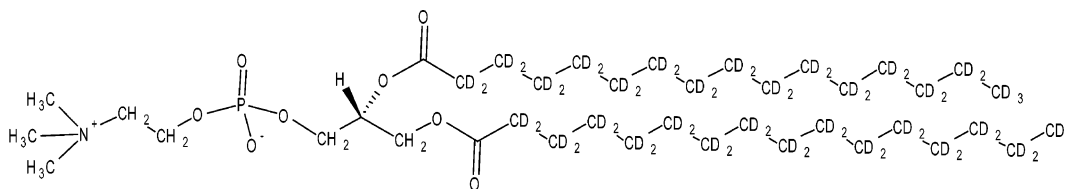
(67) Guyot-Sionnest, P.; Hunt, J. H.; Shen, Y. R. *Phys. Rev. Lett.* **1987**, *59*, 1597.

(68) Miranda, P. B.; Shen, Y. R. *J. Phys. Chem. B* **1999**, *103*, 3292.

(69) Allen, H. C.; Raymond, E. A.; Richmond, G. L. *Curr. Opin. Colloid Interface Sci.* **2000**, *5*, 74.

(70) Shultz, M. J.; Schnitzer, C.; Simonelli, D.; Baldelli, S. *Int. Rev. Phys. Chem.* **2000**, *19*, 123.

(71) Richmond, G. L. *Chem. Rev.* **2002**, *102*, 2693.

Scheme 1. Deuterated DPPC Molecule (DPPC-*d*₆₂)

monolayers have focused on the chain ordering of the DPPC tail groups. Watry et al. studied a series of phospholipid monolayers at the air–water interface with SFG and found that the chain ordering of a phospholipid monolayer was dominated by the length of the acyl chain rather than the type of headgroup.⁷³ Roke et al. used SFG to investigate the phase behavior of a DPPC monolayer and discovered a new DPPC phase transition.⁷⁴ The novel phase transition was attributed to the uncurling of the DPPC tails upon compression. To date, there is a paucity of SFG studies of DPPC monolayers that investigate both the tail and the head groups. Vibrational frequencies of certain headgroup moieties are typically in the fingerprint region (1400–800 cm⁻¹), yet SFG studies in the fingerprint region are rare.^{66,75–77} The work presented here explores both the tail and the head groups of the DPPC molecule by using chain-deuterated DPPC (DPPC-*d*₆₂) and by tuning the infrared laser pulse to cover different vibrational frequency regions including the fingerprint region. We provide a comprehensive picture of the interfacial behavior of DPPC in different thermodynamic phases and elucidate fundamental issues such as chain conformation, chain orientation, headgroup orientation, and headgroup hydration.

A brief description of the SFG approach as well as the SFG theory is provided as follows. SFG utilizes two pulsed laser beams of different frequencies, which generate a third frequency at the sum of the two probing beams' frequencies. Usually, one beam is in the visible region, and the other is in the infrared region. When the infrared pulse is resonant with a vibrational mode of the molecule adsorbed at the surface, there will be an SFG signal enhancement. The enhanced signal provides a surface vibrational spectrum. SFG has all of the advantages of FTIR and Raman, yet it is also surface-selective. The surface selectivity comes from a unique selection rule requiring the lack of inversion symmetry. The interface always satisfies this selection rule, but the isotropic bulk does not.

A brief description of the theory of SFG is outlined here. Details can be found in the literature.^{78–85} The SFG intensity, I_{SFG} , as shown in eq 1,

$$I_{\text{SFG}} \propto |\chi^{(2)}|^2 \propto |\chi_{\text{NR}}^{(2)} + \sum_v \chi_v^{(2)}|^2 \quad (1)$$

(72) Chen, Z.; Shen, Y. R.; Somorjai, G. A. *Annu. Rev. Phys. Chem.* **2002**, *53*, 437.

(73) Watry, M. R.; Tarbuck, T. L.; Richmond, G. L. *J. Phys. Chem. B* **2003**, *107*, 512.

(74) Roke, S.; Schins, J.; Muller, M.; Bonn, M. *Phys. Rev. Lett.* **2003**, *90*, 128101/1.

(75) Johnson, C. M.; Tyrode, E.; Baldelli, S.; Rutland, M. W.; Leygraf, C. J. *Phys. Chem. B* **2005**, *109*, 321.

(76) Hore, D. K.; Beaman, D. K.; Richmond, G. L. *J. Am. Chem. Soc.* **2005**, *127*, 9356.

(77) Hore, D. K.; Beaman, D. K.; Parks, D. H.; Richmond, G. L. *J. Phys. Chem. B* **2005**, *109*, 16846.

(78) Dick, B.; Gierulski, A.; Marowsky, G. *Appl. Phys. B* **1985**, *38*, 107.

(79) Hirose, C.; Akamatsu, N.; Domen, K. *Appl. Spectrosc.* **1992**, *46*, 1051.

(80) Hirose, C.; Yamamoto, H.; Akamatsu, N.; Domen, K. *J. Phys. Chem.* **1993**, *97*, 10064.

(81) Zhuang, X.; Miranda, P. B.; Kim, D.; Shen, Y. R. *Phys. Rev. B* **1999**, *59*, 12632.

(82) Moad, A. J.; Simpson, G. J. *J. Phys. Chem. B* **2004**, *108*, 3548.

(83) Wang, J.; Clarke, M. L.; Chen, Z. *Anal. Chem.* **2004**, *76*, 2159.

is proportional to the absolute square of the macroscopic second-order nonlinear susceptibility, $\chi^{(2)}$, which consists of resonant terms ($\chi_v^{(2)}$) and a nonresonant term ($\chi_{\text{NR}}^{(2)}$). When the frequency of an incident infrared beam, ω_{IR} , is resonant with a surface vibrational mode, ν , then the resonant susceptibility term ($\chi_v^{(2)}$) dominates the nonlinear susceptibility ($\chi^{(2)}$), and an SFG intensity enhancement is observed. The resonant macroscopic nonlinear susceptibility, $\chi_v^{(2)}$, is shown in eq 2

$$\chi_v^{(2)} \propto \frac{A_\nu}{\omega_{\text{IR}} - \omega_\nu + i\Gamma_\nu} \quad (2)$$

where A_ν is the strength of the transition moment, ν is the frequency of the transition moment, and Γ_ν is the line width of the transition. The amplitude, A_ν , is nonzero when the Raman and the infrared transitions are both spectroscopically allowed. $\chi_v^{(2)}$ is related to the molecular hyperpolarizability, β_ν , shown in eq 3, by the number density of the surface species, N , and an orientationally averaged Euler angle transformation $\langle \mu_{IJK:lmn} \rangle$ between the laboratory coordinates (I, J, K) and the molecule coordinates (l, m, n).

$$\chi_v^{(2)} = N \sum_{lmn} \langle \mu_{IJK:lmn} \rangle \beta_\nu \quad (3)$$

Experimental Section

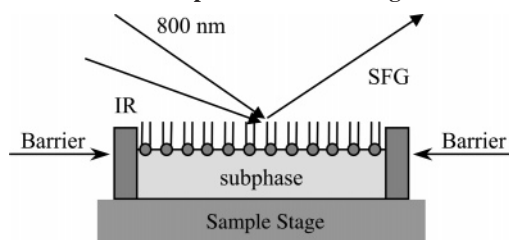
Materials. Acyl-chain-deuterated 1,2-dipalmitoyl-*sn*-glycero-3-phosphocholine (as shown in Scheme 1) with >99% purity was obtained from Avanti Polar Lipids (Alabaster, AL) and used without further purification. Spectral-grade chloroform was purchased from Sigma-Aldrich Chemical Co. (St. Louis, MO). Deionized water from a Barnstead Nanopure system with a resistivity of 18.2 M Ω ·cm was used.

Methods. *Langmuir Film Balance.* The surface pressure–area isotherm was obtained with a KSV minitrough (KSV, Finland). The rectangular trough (176.5 mm \times 85 mm) is made of Teflon and is thermostated by circulating water in channels placed underneath the trough at a temperature of 24 ± 0.5 °C. Two barriers are employed to provide symmetric film compression. The barriers are made of Delrin, a hydrophilic material that prevents monolayer leakage beneath the barriers. The surface pressure and the mean molecular area are continuously monitored during film compression by the Wilhelmy plate method. The plate is made of platinum and is flamed with a Bunsen burner before use. The trough is filled with pure water as the subphase. The surface pressure–area isotherm is always measured on a fresh subphase. The clean subphase surface is swept by barriers to make sure that there is no significant surface pressure increase observed upon compression. A stock chloroform solution of DPPC-*d*₆₂ with a concentration of 1 mM was used. The solution was kept in a freezer at -20 °C when not being used. A known amount of DPPC solution was spread on the subphase surface in a dropwise manner with a Hamilton syringe, and 10 min was allowed to elapse for complete solvent evaporation before starting the

(84) Wang, H.-F.; Gan, W.; Lu, R.; Rao, Y.; Wu, B.-H. *Int. Rev. Phys. Chem.* **2005**, *24*, 191.

(85) Lambert, A. G.; Davies, P. B.; Neivandt, D. J. *Appl. Spectrosc. Rev.* **2005**, *40*, 103.

Scheme 2. SFG Experiment on a Langmuir Trough



compression. A constant compression speed of 10 mm/min (corresponding to a 5 mm/min barrier moving speed) was used.

Broad Bandwidth Sum Frequency Generation Spectroscopy. Details of the broad bandwidth sum frequency generation (BBSFG) system can be found elsewhere.^{86,87} A brief description is given below. Two 1-kHz repetition rate regenerative amplifiers (Spectra-Physics Spitfire, femtosecond and picosecond versions) are utilized in the BBSFG setup. The picosecond amplifier produces a narrow bandwidth (17 cm^{-1}) 2 ps pulse at a wavelength of $\sim 800\text{ nm}$. The femtosecond amplifier is used to pump an optical parametric amplifier (OPA; Spectra-Physics OPA-800F) to produce a broad bandwidth of $\sim 100\text{ fs}$ infrared pulse. The spectral window of the broad IR pulse can be as large as 500 cm^{-1} , depending on the tuned spectral region. Therefore, in a BBSFG system, an SFG spectrum can be obtained without wavelength scanning. Tuning the nonlinear crystals cooperatively in the OPA allows the system to cover different wavelength regions such as the C–H stretching region ($2700\text{--}3000\text{ cm}^{-1}$), the C–D stretching region ($2000\text{--}2300\text{ cm}^{-1}$), and the PO_2^- symmetric stretching region ($1000\text{--}1200\text{ cm}^{-1}$). The input energy of the 800 nm beam is $300\text{ }\mu\text{J}$. The IR energies are $9\text{ }\mu\text{J}$ in the C–H stretching region, $6\text{ }\mu\text{J}$ in the C–D stretching region, and $1\text{ }\mu\text{J}$ in the PO_2^- symmetric stretching region.

The BBSFG experiment is performed in reflection geometry. The miniature design of the KSV minitrough makes the trough well suited to the relatively small space of the sample area. The Langmuir film balance, as shown in Scheme 2, is placed on the sample stage of the BBSFG system. The stage has a z -axis translator, and the height of the monolayer surface in the Langmuir trough can be accurately adjusted vertically. The two probe beams (800 nm and IR) are overlapped at the monolayer surface spatially and temporally. The generated SFG signal, containing spectral information from the surface, is detected by a monochromator CCD detection system. Because the infrared pulse is broadband, an SFG spectrum is obtained. The SFG spectrum is polarization-dependent. In this study, three polarization combinations are used: ssp (s-SFG; s-800 nm; p-infrared), ppp (p-SFG; p-800 nm; p-infrared), and sps (s-SFG; p-800 nm; s-infrared). Changing polarizations from s to p can be obtained by using a zero-order waveplate in the 800 nm beam line and a MgF_2 Berek's compensator in the IR beam line (for the C–H and C–D stretching regions). A Glan laser polarizer selects the polarization in the SFG detection system. The SFG spectrum is normalized against a nonresonant SFG spectrum from a GaAs crystal to remove the spectral distortion caused by the energy profile of the infrared pulse. The normalization process also makes it possible to compare the SFG spectra taken by different SFG systems.

When performing the SFG study on the monolayer, the monolayer is first compressed by the two barriers to reach a given surface pressure. The barriers are then halted, and an SFG spectrum is obtained. During the 5 min spectral acquisition time, the monolayer relaxes, and a surface pressure drop occurs. The surface pressure drop was also observed by other researchers when performing IRRAS studies on DPPC-containing monolayers.^{46,47} The largest pressure drop during the 5 min spectral acquisition is less than 6 mN/m , and this occurs when DPPC is compressed into the liquid-condensed phase. To ensure that the surface pressure drop does not produce an artifact in the SFG spectrum, the surface was monitored for 5 min by taking 10 consecutive BBSFG spectra with a 30 s acquisition

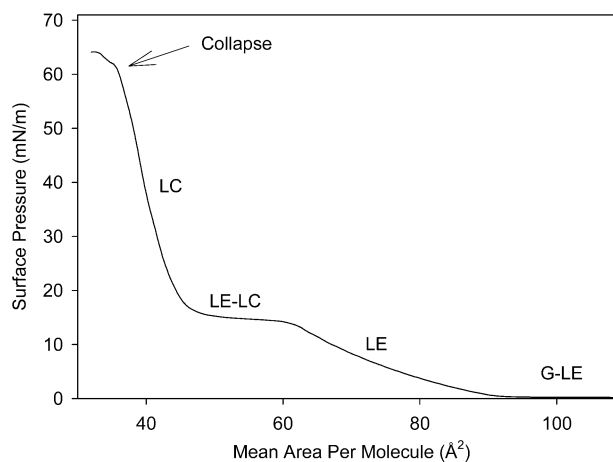


Figure 1. Surface pressure (mN/m)–area (\AA^2) isotherm of deuterated DPPC- d_{62} at $24\text{ }^\circ\text{C}$ on a pure-water subphase. G: gas phase; LE: liquid-expanded phase; LC: liquid-condensed phase; G–LE: coexistence of G and LE phases; LE–LC: coexistence of LE and LC phases.

time in real time during the surface pressure drop. The 10 30-s BBSFG spectra were found to be identical, implying that the surface pressure drop had a negligible effect on the SFG spectrum.

In this article, we show representative SFG spectra obtained at 1, 12, and 42 mN/m ; however, numerous SFG spectra were obtained along the entire isotherm. The SFG spectra of the monolayer are fit with Lorentzian line shapes according to eqs 1 and 2 using IGOR commercial software after adding additional codes to describe the coherent nature of the SFG process as shown in eq 1.

Results and Discussion

Isotherm of DPPC- d_{62} . Surface pressure–area isotherm measurements are the conventional way to characterize the phase behavior of Langmuir monolayers.⁸⁸ Figure 1 shows the surface pressure–area isotherm of deuterated DPPC- d_{62} at $24\text{ }^\circ\text{C}$ on a pure water subphase. A number of distinct regions are shown in this isotherm. Each region is a separate phase.⁸⁸ These phases are functions of surface pressure, surface area, and temperature. Following the general assignments for the phospholipid phases in the literature,⁸⁹ these phases have been assigned as G–LE, LE, LE–LC, LC, and collapse phases as denoted in Figure 1. G is the gas phase; LE is the liquid expanded phase; LC is the liquid condensed phase (or TC, tilted-condensed⁸⁹); G–LE is the coexistence of G and LE; and LE–LC is the coexistence of LE and LC.

Molecules in the gas phase are loosely packed at the water surface and behave like a 2D gas. As the monolayer is being compressed, there is a G–LE transition (the first plateau to the far right in the isotherm). In the LE phase, molecules behave like a 2D liquid and are not as free to move about as in the gas phase. As the monolayer is being compressed further, the LE–LC phase transition (the second plateau when reading from right to left in the isotherm) will occur. The LE–LC phase transition occurs at $\sim 15\text{ mN/m}$ for DPPC- d_{62} , about 10 mN/m higher than that of nondeuterated DPPC. The high LE–LC phase-transition pressure of DPPC- d_{62} is consistent with a previous study.⁴¹ In the LC phase, molecules are in a 2D semicrystalline phase. Further compression results in film collapse at a surface pressure of 63 mN/m , where a kink appears in the isotherm. (The collapse pressure of DPPC can be above 70 mN/m if the Langmuir trough is equipped with a ribbon barrier.⁹)

(86) Ma, G.; Allen, H. C. *J. Phys. Chem. B* **2003**, *107*, 6343.

(87) Ma, G.; Liu, D.; Allen, H. C. *Langmuir* **2004**, *20*, 11620.

(88) Gaines, G. L. *Insoluble Monolayers at Liquid–Gas Interfaces*; Interscience Publishers: New York, 1966.

(89) Kaganer, V. M.; Möhwald, H.; Dutta, P. *Rev. Mod. Phys.* **1999**, *71*, 779.

Table 1. Fitted Peak Frequencies and Assignments of the BBSFG Spectra of DPPC-*d*₆₂ at Different Surface Pressures^a

	CD ₃ -SS (cm ⁻¹)	CD ₂ -SS (cm ⁻¹)	CD ₃ -FR (cm ⁻¹)	CD ₂ -AS (cm ⁻¹)	CD ₃ -AS (cm ⁻¹)	CH ₂ -SS (cm ⁻¹)	CH ₃ -SS (cm ⁻¹)	PO ₂ ⁻ -SS (cm ⁻¹)
1 mN/m (LE)	2071	2105		2195	2218			
12 mN/m (LE)	2073	2102	2121	2194	2221	2912	2958	1094
42 mN/m (LC)	2071		2123		2221	2912	2959	1104

^a SS: symmetric stretch; AS: asymmetric stretch; FR: Fermi resonance.

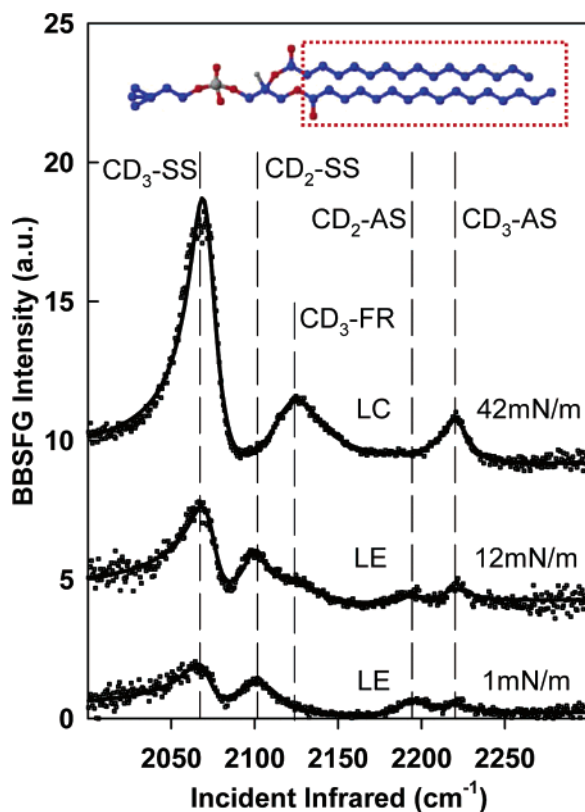


Figure 2. ssp BBSFG spectra of the DPPC-*d*₆₂ monolayer in the C–D stretching region at different surface pressures. Solid lines are spectral fits. Dashed vertical lines reveal the spectral assignments: SS, symmetric stretch; FR, Fermi resonance; AS, asymmetric stretch.

Conformation and Orientation of DPPC-*d*₆₂ Tail Groups.

The surface pressure–area isotherm provides thermodynamic information about the monolayer. Vibrational sum frequency generation spectroscopy is used to gain additional molecular-level insight. Figure 2 shows the BBSFG spectra of DPPC-*d*₆₂ with ssp polarization at three different surface pressures: 1, 12, and 42 mN/m. The spectra were obtained in the C–D stretching region and provide information about the conformation and orientation of the deuterated DPPC tails. Table 1 lists the peak positions from curve fits and the spectral assignments. At 1 mN/m, there are four peaks revealed in the spectrum located at 2071, 2105, 2195, and 2218 cm⁻¹ as listed in Table 1. According to previous vibrational spectroscopic studies on deuterated DPPC and relevant compounds,^{90–93} these four peaks are assigned to CD₃ symmetric stretch (CD₃-SS), CD₂ symmetric stretch (CD₂-SS), CD₂ asymmetric stretch (CD₂-AS), and CD₃ asymmetric stretch (CD₃-AS) modes, respectively. At 12 mN/m, an

additional shoulder is observed at 2121 cm⁻¹ and is assigned to the CD₃ Fermi resonance (CD₃-FR). At 42 mN/m, only three peaks—the CD₃-SS, CD₃-FR, and CD₃-AS—are observed in the BBSFG spectrum.

SFG spectroscopy is a sensitive surface technique that can detect the conformation change and the orientation change of a surface-adsorbed molecule. First, the SFG selection rule is employed to gain conformation information about the DPPC tails at the air–water interface from Figure 2. As shown in Figure 2, at either 1 or 12 mN/m the peaks from the methylene groups (CD₂-SS and CD₂-AS) are clearly observed in the BBSFG spectra. This is a clear indication of the existence of gauche configurations adopted by the DPPC tails. Recall the selection rule of lack of inversion symmetry mentioned in the Introduction; its application is well demonstrated by Figure 2. At 1 or 12 mN/m, DPPC is in the LE phase and behaves as a 2D liquid. The fluidity of this phase causes the hydrocarbon tails to become disordered and adopt flexible gauche configurations. The lack of inversion symmetry between each pair of gauche methylene groups allows both the CD₂-SS and the CD₂-AS peaks to be SFG-active; therefore, the two peaks are clearly observed in the BBSFG spectra of 1 and 12 mN/m. At 42 mN/m, both the CD₂-SS and the CD₂-AS peaks disappear from the BBSFG spectrum, implying that the DPPC tails adopt an all-trans configuration in the LC phase. The all-trans configuration creates inversion symmetry between trans pairs of methylene groups. Because there are even numbers of methylene groups in the DPPC tail, no single methylene can be SFG-active; therefore, both the CD₂-SS and CD₂-AS peaks disappear, and only the CD₃-SS, CD₃-FR, and CD₃-AS peaks are observed in the BBSFG spectrum at 42 mN/m.

The unique selection rule, with respect to inversion symmetry, makes SFG a valuable tool for investigating the lipid chain conformation. This is particularly helpful because most biorelevant lipids have even numbers of methylene groups in their hydrocarbon chains.⁹⁴ This is especially true for lung surfactant lipid components.⁴ The appearance and disappearance of methylene (CD₂) SFG intensity is essentially a binary indicator that easily and accurately shows the presence and absence of the gauche conformation in the hydrocarbon chains.

There is a large body of pioneering work on Langmuir monolayers with IRRAS by Dluhy and Mendelsohn and co-workers in lung surfactant and biomembrane research.^{43–51,95,96} It is important to note that the lack of inversion symmetry selection rule is a distinct feature of SFG as compared with IRRAS; therefore, these techniques are complementary as opposed to duplicative. Given an example, an all-trans hydrocarbon chain of a lipid molecule with an even number of methylene groups will produce a strong signal in the methylene stretching region in the IRRAS spectrum but will produce no signal in the SFG spectrum because there are inversion centers for each trans pair of methylene groups.

(90) Duncan, J. L.; Kelly, R. A.; Nivellini, G. D.; Tullini, F. *J. Mol. Spectrosc.* **1983**, *98*, 87.

(91) Sunder, S.; Cameron, D. G.; Casal, H. L.; Boulanger, Y.; Mantsch, H. H. *Chem. Phys. Lipids* **1981**, *28*, 137.

(92) Devlin, M. T.; Levin, I. W. *J. Raman Spectrosc.* **1990**, *21*, 441.

(93) Zhang, D.; Gutow, J.; Eisenthal, K. B. *J. Phys. Chem.* **1994**, *98*, 13729.

(94) Gennis, R. B. *Biomembranes: Molecular Structure and Function*; Springer-Verlag: New York, 1989.

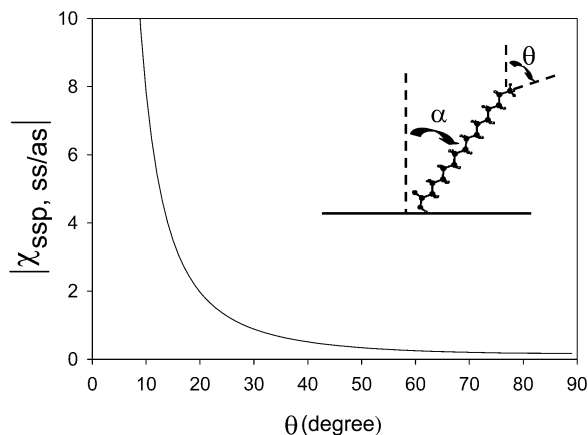


Figure 3. Square root of the ratio between the SFG intensities of CD₃-SS and CD₃-AS as a function of the mean orientation angle θ . (Inset) Illustration of the mean orientation angle θ and the chain tilt angle α .

Another valuable piece of information that can be obtained from Figure 2 is the orientation angle of the terminal methyl group. The angle can also be used to deduce the chain tilt angle of DPPC with respect to the surface normal. SFG orientation calculation methods have been well documented in the literature.^{78–85} Briefly, the functional relationship between the SFG second-order nonlinear susceptibility (χ) and the mean orientation angle (θ) forms the mathematical basis for the orientation calculation. The procedure requires solving simultaneous equations because θ is not the only unknown parameter. In the case of DPPC-*d*₆₂, the orientation angle of the terminal CD₃ group (i.e., the tilt angle of the C_{3v} axis of CD₃ from the surface normal) is calculated in the following way:

$$\chi_{yyz}(\text{CD}_3\text{-SS}) = \frac{1}{2}N\beta_{\text{ccc}}[\cos\theta(1+r) - \cos^3\theta(1-r)]$$

$$r = \frac{\beta_{\text{aac}}}{\beta_{\text{ccc}}} \quad (4)$$

$$\chi_{yyz}(\text{CD}_3\text{-AS}) = -N\beta_{\text{caa}}(\cos\theta - \cos^3\theta) \quad (5)$$

The second-order nonlinear susceptibility (χ) of CD₃-SS and CD₃-AS are related to θ , the surface molecular density N , and the molecular hyperpolarizability β as described in eqs 4 and 5, where the ssp polarization combination is used during the SFG measurement. As shown in Figure 3, the ratio between $\chi_{yyz}(\text{CD}_3\text{-SS})$ and $\chi_{yyz}(\text{CD}_3\text{-AS})$ has a direct relationship with θ (values of $r = 2.3$ (ref 93) and $\beta_{\text{caa}}/\beta_{\text{aac}} = 4.2$ (ref 97)). Therefore, θ can be easily obtained by knowing the ratio of $\chi_{yyz}(\text{CD}_3\text{-SS})$ to $\chi_{yyz}(\text{CD}_3\text{-AS})$. In practice, this ratio is obtained from the square root of the ratio of CD₃-SS to CD₃-AS peak intensities. To use the above method, it is necessary to assume that the CD₃ group has C_{3v} symmetry, the surface is isotropic, and the orientation distribution is a δ function. If we assume a Gaussian distribution, then the orientation calculation becomes additionally complicated.⁹⁸

The calculated θ values of the terminal methyl groups are listed in Table 2. In the all-trans methylene configuration, the angle relationship between the chain axis and the terminal methyl is known to be about 41.5° (which is the average angle of the

Table 2. Mean CD₃ Orientation Angles θ and Chain Tilt Angle α Obtained from the BBSFG Spectra of DPPC-*d*₆₂ at Different Surface Pressures

DPPC- <i>d</i> ₆₂	θ (CD ₃ orientation angle)	α (chain tilt angle) ^a
1 (mN/m) (LE)	15.6 ± 1.0°	
12 (mN/m) (LE)	15.8 ± 1.8°	
42 (mN/m) (LC)	16.4 ± 0.9°	25°

$$^a \alpha = 41.5^\circ - \theta.$$

two chains deduced from the literature⁷⁴). Therefore, the chain tilt angle α with respect to the surface normal can be easily deduced from the relationship of $\alpha = 41.5^\circ - \theta$.⁹⁹ As shown in Table 2, the calculated value is 25° in the LC phase. The calculation with SFG is in good agreement with the previous results from X-ray diffraction studies,^{38,100} an IRRAS study,¹⁰¹ and computer simulation.¹⁰² The fact that the DPPC tails must tilt in the condensed phase (i.e., a close-packed environment) has been established.^{94,103,104} The tilt is thought to be due to the space requirement mismatch between the head and the tail. In the DPPC molecule, the size of the headgroup is relatively large. According to a previous X-ray study on phospholipids,¹⁰³ the surface area occupied by the bulky headgroup of the PC is about 50 Å². However, the minimum cross-sectional area of the two hydrocarbon chains of the PC is about 38 Å². In a close-packed environment, as in the LC phase, the chain must be tilted to some extent to compensate for the head–tail mismatch to form a stable monolayer at the air–water interface.

Data in Table 2 also reveal another interesting phenomenon. When in different phases (LE and LC) and under different surface pressures (1, 12, and 42 mN/m), the orientation angles of the terminal methyl groups remain basically unchanged. As mentioned earlier, at 1 and 12 mN/m, the DPPC tails adopt gauche configurations. If there is only a single gauche configuration in the chain, then when the chain becomes all-trans (...ttt...) the orientation of the terminal methyl group will change. However, if the gauche configurations are in the g⁺tg⁻ (first-order kink) or g⁺ttg⁻ (second-order kink) or g⁺tg⁻tg⁺ (second order kink) configuration, as shown in Scheme 3, then this only horizontally displaces the top and bottom portion of the chain.¹⁰⁵ In this way, as the monolayer is compressed, the elimination of the gauche configurations will not change the orientation of the terminal methyl groups. However, two experimental details revealed in Figure 2 argue against the above explanation. First, kink configurations, as shown in Scheme 3, retain the inversion symmetry between the methylene groups.¹⁰⁶ This means that both the CD₂-SS and the CD₂-AS peaks will disappear from the BBSFG spectra of 1 and 12 mN/m according to the selection rule of SFG. Clearly, this is not the case in Figure 2; both the CD₂-SS and the CD₂-AS peaks exist in the BBSFG spectra of 1 and 12 mN/m. Second, Figure 4 illustrates the relationship between the surface molecular density N and the square root of the area of

(99) Ye, S.; Noda, H.; Nishida, T.; Morita, S.; Osawa, M. *Langmuir* **2004**, *20*, 357.

(100) Brezesinski, G.; Dietrich, A.; Struth, B.; Boehm, C.; Bouwman, W. G.; Kjaer, K.; Möhwald, H. *Chem. Phys. Lipids* **1995**, *76*, 145.

(101) Gericke, A.; Flach, C. R.; Mendelsohn, R. *Biophys. J.* **1997**, *73*, 492.

(102) Dominguez, H.; Smondryev, A. M.; Berkowitz, M. L. *J. Phys. Chem. B* **1999**, *103*, 9582.

(103) Hauser, H.; Pascher, I.; Pearson, R. H.; Sundell, S. *Biochim. Biophys. Acta* **1981**, *650*, 21.

(104) Möhwald, H. *Annu. Rev. Phys. Chem.* **1990**, *41*, 441.

(105) Lagaly, G.; Weiss, A.; Stuke, E. *Biochim. Biophys. Acta* **1977**, *470*, 331.

(106) Goates, S. R.; Schofield, D. A.; Bain, C. D. *Langmuir* **1999**, *15*, 1400.

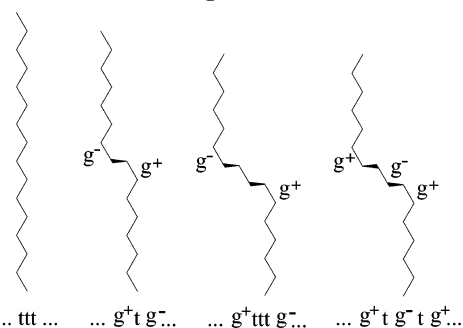
(95) Dluhy, R. A.; Cornell, D. G. *J. Phys. Chem.* **1985**, *89*, 3195.

(96) Mitchell, M. L.; Dluhy, R. A. *J. Am. Chem. Soc.* **1988**, *110*, 712.

(97) Wang, C.-Y.; Groenzin, H.; Shultz, M. J. *J. Phys. Chem. B* **2004**, *108*, 265.

(98) Wang, J.; Paszti, Z.; Even, M. A.; Chen, Z. *J. Am. Chem. Soc.* **2002**, *124*, 7016.

Scheme 3. Hydrocarbon Chain in Different Conformation Configurations^a



^a All-trans chain and kinked chains.

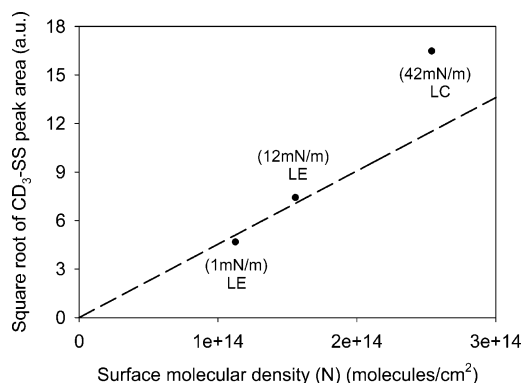


Figure 4. Relationship between the square root of the fit peak area of CD₃-SS in Figure 2 and the surface molecular density *N*. The dashed line shows a proportional relationship between *N* and the square root of the peak area of the CD₃ group.

the CD₃-SS peak for the three surface pressures: 1, 12, and 42 mN/m. A disproportional increase in the square root of the CD₃-SS peak area is observed at 42 mN/m (with the 42 mN/m data point deviating from the dashed line). The disproportional CD₃ intensity increase of the LC phase as compared with the LE phase suggests that the orientational ordering of the terminal methyl group in the LE phase is different from that of the LC phase.⁶⁷ This contradicts the situation described in Scheme 3, where the orientational ordering of the terminal CD₃ group remains unchanged when the hydrocarbon chain turns from a kink configuration into an all-trans configuration. On the basis of the two points stated above, we assert that the lack of variation of the CD₃ orientation angle as shown in Table 2 is due to the fact that the CD₃ mean orientation angle is insensitive to the surface pressure variation and LE–LC phase transition, though the DPPC chain in the LE phase can possibly adopt a variety of gauche configurations.

Orientation of the Choline Headgroup. The headgroup orientation of phosphatidylcholine is generally referred to as the inclination angle of the P–N dipole moment (P and N are the phosphorus and nitrogen atoms of the headgroup) with respect to the surface.¹⁰³ Numerous studies have been completed on phospholipid bilayer systems, and it has been suggested that the P–N dipole lies flat with respect to the bilayer surface.⁹⁴ As for the DPPC monolayer, there is little evidence available in the literature of the actual orientation of the P–N dipole. Surface potential measurements suggest that the headgroup orientation in the monolayer is parallel to the air–water interface.¹⁰⁴ A previous computer simulation investigation on a DPPC monolayer showed that the average angle between the water surface and the P–N dipole was 5°. ¹⁰²

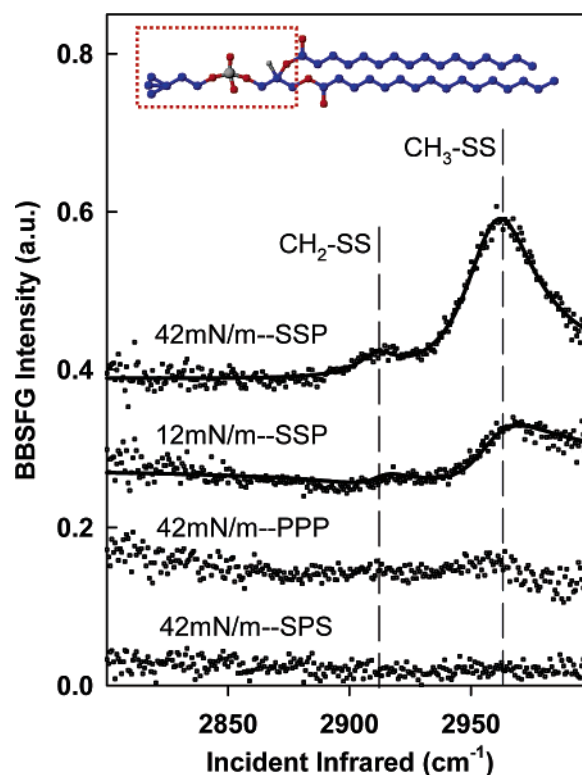
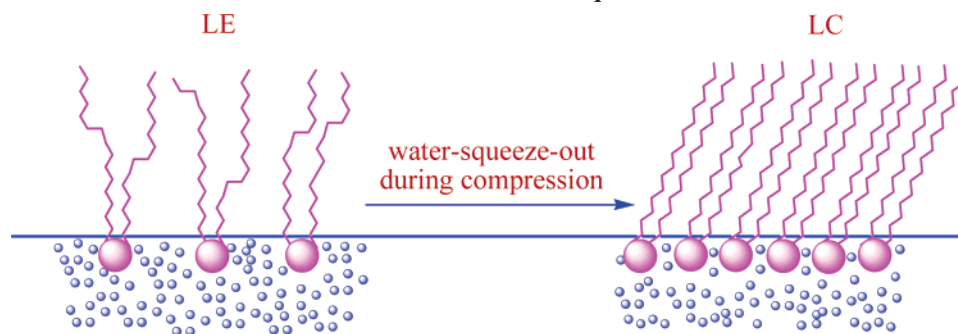


Figure 5. ssp, ppp, and sps BBSFG spectra of the DPPC-*d*₆₂ monolayer in the C–H stretching region at two different surface pressures. Solid lines are spectral fits. Dashed vertical lines indicate the spectral peak positions and assignments.

An SFG investigation of the choline methyl groups offers insight from a spectroscopic view. As shown in Figure 5 and Table 1, the choline methyl groups are investigated at surface pressures of 12 and 42 mN/m in the C–H stretching region. Three polarization combination measurements (ssp, ppp, and sps) are performed. In the two ssp spectra, peaks are observed at 2912 cm⁻¹ and 2959 cm⁻¹; in the ppp spectrum, the two peaks are barely visible; in the sps spectrum, no peaks are observed. Using polarization selection guidelines presented by Wang and coworkers, that is, CH₂-SS and CH₃-SS peak intensities in ssp spectra are always stronger relative to ppp,⁸⁴ the two observed peaks in Figure 5 are assigned to the CH₂-SS and the CH₃-SS modes as listed in Table 1. The CH₂-SS can originate from the glycerol backbone, the choline group, or both. The CH₃-SS peak is assigned to the choline methyl groups. The near disappearance of the CH₃-SS in the ppp spectrum makes it difficult to quantitatively analyze the orientation angle of the choline methyl groups. However, this spectral feature along with the ssp intensity qualitatively suggests that the three choline methyl groups are tilted from the surface normal and lie somewhat parallel to the air–water interface.⁸⁴

Another feature of Figure 5 is that the two spectra at 12 mN/m (LE phase) and 42 mN/m (LC phase) are rather similar. This suggests that the choline headgroup orientation is not significantly different in the LC and LE phases. This observation appears to be consistent with the conclusion drawn from a previous X-ray crystallographic study on phosphatidylcholine. The overall conformation of the polar region of phosphatidylcholine appears to be independent of the aggregation state and the nature of the environment.¹⁰³

Hydration of the Phosphate Headgroup. The structural difference between the LE and LC phases is also revealed by the hydration state of the phosphate group. Figure 6 shows the PO₂⁻ symmetric stretch (PO₂⁻-SS) of DPPC in the LE and LC phases.

Scheme 4. Illustration of the Water-Squeeze-Out Process^a

^a Blue dots represent water molecules. Possible chain conformations and orientations in the LE phase are shown.

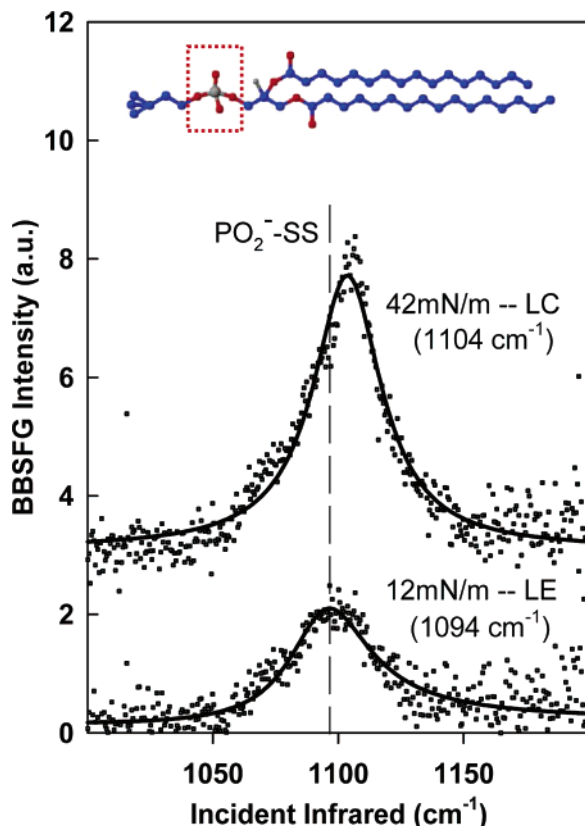


Figure 6. ssp BBSFG spectra of the DPPC-*d*₆₂ monolayer in the fingerprint region at two different surface pressures. Solid lines are the spectral fits. Dashed vertical lines reveal the peak position of the PO₂⁻ symmetric stretch in the LE phase. There is a 10 cm⁻¹ shift to higher energy upon compression to the LC phase.

The peak position and assignment are listed in Table 1. The assignment is unambiguous from the literature.^{107–109} As shown in Figure 6, the PO₂⁻SS peak is observed at 1094 cm⁻¹ in the LE phase and shifts to 1104 cm⁻¹ in the LC phase. The shift to a higher frequency indicates that the hydration environment of the phosphate group changes as a result of monolayer compression.

Phosphate hydration is a crucial factor affecting the interfacial behavior of phospholipids. Even so, the headgroup conformation and hydration are poorly understood, particularly when compared to the level of understanding of the DPPC tail. To our knowledge,

the SFG spectrum shown here is the first SFG vibrational spectrum from a phospholipid phosphate group. The frequency shift observed in Figure 6 can be easily explained with the so-called water-squeeze-out mechanism as illustrated in Scheme 4. In the LE phase, DPPC molecules are loosely packed, and the headgroup occupies a large area at the air–water interface. The phosphate group is well solvated by interfacial water molecules. The hydrogen bonding network between water molecules and the phosphate group weakens the PO₂⁻ bonds and causes the vibrational frequency to shift to a lower wavenumber (1094 cm⁻¹) relative to that of the LC phase. In the LC phase, the close packing of DPPC requires the water in the hydration shell to be squeezed out by compression. The less hydrated state of the phosphate group causes the PO₂⁻ bond to be strengthened; consequently, its vibrational frequency is observed at a higher wavenumber (1104 cm⁻¹) relative to that of the LE phase. The infrared frequency shift of the DPPC PO₂⁻ symmetric stretch, which is due to the change in hydration state, has been well documented in previous infrared studies on DPPC in the bulk phase.^{110,111} A recent quantum chemical calculation on an analogous molecule of methylphosphocholine (MePC) has revealed atomic-level details of the cause of the phosphate frequency shift upon hydration.¹¹² It has been shown that hydration of the phosphate group induces the loss of electron density of the PO₂⁻ bonds due to strong hyperconjugation with the O–H antibonding orbital of water and weakens the PO₂⁻ bonds.

The occurrence of water squeeze out at the air–water interface in Langmuir monolayers has been long postulated by Langmuir, Schulman, Hughes,⁸⁸ and Figure 6 shows direct experimental evidence of this phenomenon. Previously, this phenomenon was also observed from a deuterated long-chain cyanide (CD₃(CH₂)₁₉-CN) with SFG at the air–water interface by Eisenthal and co-workers.⁹³

Implications for Lung Surfactant Function. It has been shown clinically that DPPC alone fails to be an effective replacement surfactant mainly because of its poor respreading and adsorption abilities.⁴ Phosphate hydration, as shown in the present study, provides molecular-level insight into why DPPC respreads poorly; that is, the phosphate group is significantly affected during compression as dehydration is occurring. We postulate that the poor respreading property of DPPC in the LC phase is due to its headgroup hydration state. The poor hydration property of DPPC in the LC phase at the air–water interface is somewhat similar to the poor swelling property of DPPC in

(107) Arrondo, J. L.; Goni, F. M.; Macarulla, J. M. *Biochim. Biophys. Acta* **1984**, *794*, 165.

(108) Okamura, E.; Umemura, J.; Takenaka, T. *Biochim. Biophys. Acta* **1990**, *1025*, 94.

(109) Wong, P. T.; Capes, S. E.; Mantsch, H. H. *Biochim. Biophys. Acta* **1989**, *980*, 37.

(110) Pohle, W.; Selle, C.; Fritzsche, H.; Bohl, M. *J. Mol. Struct.* **1997**, *408/409*, 273.

(111) Gauger, D. R.; Selle, C.; Fritzsche, H.; Pohle, W. *J. Mol. Struct.* **2001**, *565/566*, 25.

(112) Mrazkova, E.; Hobza, P.; Bohl, M.; Gauger, D. R.; Pohle, W. *J. Phys. Chem. B* **2005**, *109*, 15126.

water when DPPC is in the smectic liquid crystalline phase.¹¹³ We therefore assert that headgroup hydration is a crucial factor regulating the lung surfactant interfacial behavior during inhalation and exhalation. Consequently, lipid headgroup hydration should be considered in the design of exogenous lung surfactant.

Conclusions

A comprehensive view of DPPC conformation, surface orientation, and hydration in a Langmuir monolayer at the air–water interface was presented. As the DPPC Langmuir monolayer undergoes the transition from the liquid-expanded phase to the liquid-condensed phase, the methylene groups of the DPPC tails transform from predominantly gauche conformations to all-trans conformations. Concomitantly during compression, water is

squeezed out from the hydration shell of the headgroup, leaving a less hydrated phosphate group to anchor the DPPC at the air–water interface. The phosphate group is significantly dehydrated as revealed by the change in the vibrational frequency after compression. The orientations of the terminal methyl groups remain nearly unchanged from the LE to the LC phases. The choline headgroup orientation is not significantly different in the LE and LC phases, implying that the overall conformation of the headgroup is not as sensitive to the aggregation state and the nature of the environment. Moreover, we assert that headgroup hydration is a crucial factor regulating lung surfactant interfacial behavior during inhalation and exhalation.

Acknowledgment. We acknowledge the Arnold and Mabel Beckman Foundation for funding this research through a Beckman Young Investigator Award.

(113) Hauser, H. *Biochim. Biophys. Acta* **1984**, 772, 37.